

PHYSICAL REVIEW B

CONDENSED MATTER AND MATERIALS PHYSICS

THIRD SERIES, VOLUME 57, NUMBER 14

1 APRIL 1998-II

RAPID COMMUNICATIONS

Rapid Communications are intended for the accelerated publication of important new results and are therefore given priority treatment both in the editorial office and in production. A Rapid Communication in Physical Review B may be no longer than four printed pages and must be accompanied by an abstract. Page proofs are sent to authors.

Elastic and inelastic scattering of $4d$ inner-shell electrons in $(Y,Gd)_2O_3$ studied by synchrotron-radiation excitation

A. Moewes and T. Eskildsen

Center for Advanced Microstructures and Devices, CAMD at Louisiana State University, Baton Rouge, Louisiana 70803

D. L. Ederer, J. Wang, and J. McGuire

Physics Department, Tulane University, New Orleans, Louisiana 70118

T. A. Callcott

University of Tennessee, Knoxville, Tennessee 37996

(Received 26 January 1998)

Excitations within the $4f$ shell of Gd^{3+} in $(Y,Gd)_2O_3$ are observed by resonant elastic and inelastic soft x-ray scattering with synchrotron radiation. Inelastic scattering takes place when exciting $4d^{10}4f^7 \rightarrow 4d^9 4f^8$ transitions and extends over an energy range of about 10 eV. The features can be assigned to the net transition from the $^8S_{7/2}$ ground state to the sextet multiplets of the $4f^7$ configuration in Gd^{3+} , which have the same parity as the ground state. The inelastic scattering is maximal when the excitation energy is tuned to the $4d^9 4f^8(^6D)$ intermediate state. [S0163-1829(98)51014-4]

Soft-x-ray emission (SXE) of the rare earth elements in the region of the $4d$ threshold was first investigated by Zimkina and co-workers^{1,2} using electron bombardment to excite the emission and bremsstrahlung to obtain the absorption spectra. Later, Gerken³ studied all the rare earth elements in the region 20–200 eV using photoelectron spectroscopy methods (PES) with synchrotron radiation. These investigations were followed by PES measurements in atomic vapor⁴ to investigate the partial cross sections for the inner-shell $5p$, $6s$, and $4f$ electrons. With the advent of third generation sources, SXE has been used in conjunction with inelastic photon scattering to provide new insight in understanding the electronic structure of condensed matter.^{5–7} While the rare earths have been extensively studied by PES, the availability of third generation sources have encouraged the use of SXE. Recently, SXE measurements have been extended to include the $4d$ shell of the rare earths.⁸

In this paper, we present the first measurements of ground state excitations to even parity localized final state Gd^{3+} $4f$ orbitals by high resolution soft x-ray inelastic scattering. The energy-loss mechanisms are explained by our calculations of

the energy loss spectra. We have also investigated the variation in the cross sections of these transitions with photon excitation energy. In addition to the inelastic scattering, we found that the elastic scattering profile is significantly narrower than the absorption spectrum.

Rare earth elements are characterized by their partially filled $4f$ shell. The $4f$ electrons are highly localized due to the centrifugal term in the potential and have a low binding energy (about 9 eV in Gd). When a $4d$ electron is promoted to a $4f$ state (“ $4d$ - $4f$ transition”), the strong interaction of the $4d$ vacancy with the open $4f$ shell leads to a complex multiplet structure of 37 terms in triply ionized gadolinium. Due to the strong electron correlation, these $4d$ - $4f$ transitions produce what is called the “giant resonance,” which extends over an energy range of up to 20 eV for some of the rare earth elements. In the case of gadolinium, the $4d$ ionization threshold is at 151 and 156 eV (Ref. 4), just above the “giant resonance,” whose absorption maximum is at 149 eV.

In $(Y,Gd)_2O_3$, gadolinium exists as the triply ionized atom (Gd^{3+}) due to the ionic binding to the oxygen atom.

The configuration of the outer electrons in Gd^{3+} is $4d^{10}5s^25p^64f^7$, and the half-filled $4f$ shell forms an octet ground state level of ${}^8S_{7/2}$. The ground state ${}^8S_{7/2}$ has a spherical symmetry which is very stable and therefore much less affected by the crystal field than ions with an f^6 or f^8 electron configuration. Thus atomic effects can be studied in solid Gd as has been done with absorption spectroscopy in the visible and near-UV region in different Gd-doped crystals.^{9–11} According to Zimkina and co-workers,^{1,2} who studied the $4d$ electron excitation in the rare earths by electron-beam bombardment, three transitions contribute to the emission: $4d^95p^64f^7 \rightarrow 4d^{10}5p^54f^7$ (at about 112 eV), $4d^95p^64f^8 \rightarrow 4d^{10}5p^64f^7$ (“resonant emission” at about 149 eV), and $4d^95p^64f^7 \rightarrow 4d^{10}5p^64f^6$ (emission from more highly ionized atoms at about 138 eV). The SXE spectrum obtained by electron excitation can differ greatly from that obtained by photon excitation because electrons, unlike photons, are not constrained to lose discrete quanta of energy in a scattering process.¹² In their study of inelastic scattering near the $4d$ ionization of Gd metal, Gallet *et al.*⁸ found inelastic scattering features with an energy loss of 27 eV, which, according to their interpretation, arise from transitions between the $4d^{10}5p^64f^7$ initial state and the $4d^{10}5p^54f^8$ final state and are therefore assigned to core-core transitions. Our work on Gd focuses on high resolution elastic and inelastic scattering processes that produce even parity excitations within the ground state $4f^7$ configuration.

Our experiments were performed at the beamline 8.0 of the Advanced Light Source, ALS, Lawrence Berkeley Laboratory. The undulator beamline is equipped with a spherical grating monochromator¹³ with a maximum resolving power of $E/\Delta E = 2000$. The fluorescence end station consists of a Rowland circle grating spectrometer that provides a resolving power of about 400. The incident angle of the p -polarized beam was about 10° to the sample normal.

The absorption spectrum of $(\text{Y,Gd})_2\text{O}_3$ in the region where a $4d$ inner-shell electron is promoted to a $4f$ orbit is shown in Fig. 1 (solid line). The spectrum has been taken by measuring the reflected light at the FLIPPER monochromator at HASYLAB.¹⁴ In the soft-x-ray regime, changes in the reflection spectra follow changes in the absorption spectra¹⁵ and features in both spectra appear at the same energetic position. The main peak is centered at about 149 eV and has a full width at half maximum of about 5.9 eV. The absorption obtained here is in excellent agreement with measurement of the Gd absorption obtained by Gallet *et al.* on metal⁸ and Richter *et al.*,⁴ who did not include the contribution from the elastic scattering. The absorption spectrum has been studied theoretically by several investigators, and the most recent calculations by Ogasawara and Kotani¹⁶ are in excellent agreement with the experimental observations. The spectrum represents primarily the transition from the ground state ${}^8S_{7/2}$ to the 8P level. At lower photon energies weaker features occur that result from the excitation of the core electron to the 8D and 6D levels. Transitions from the octet ground state to the sextet state become partially allowed due to the strong spin-orbit interaction.

Figure 2 shows the soft x-ray energy loss spectra in $(\text{Y,Gd})_2\text{O}_3$ in the vicinity of the $4d$ - $4f$ resonances (134–168 eV). The energy loss (or in other words the excitation energy of the final state) has been obtained by subtracting the energy

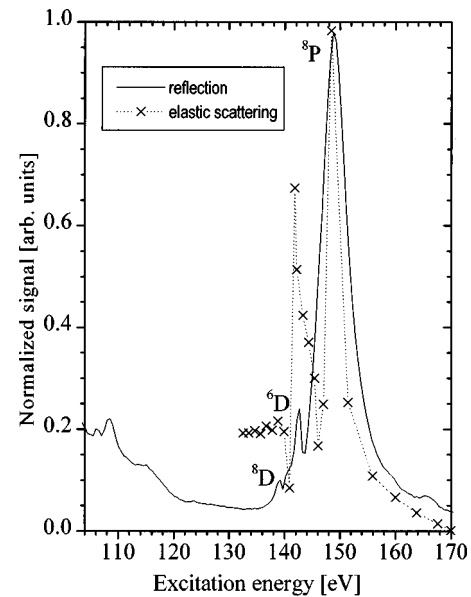


FIG. 1. Absorption spectra of $(\text{Y,Gd})_2\text{O}_3$ in the photon energy range of $4d$ - $4f$ transitions. The terms which characterize the electron configuration of the excited state ($4d^94f^8$) are given in the figure. The spectra are obtained by measuring the radiation reflected (solid line) and elastically scattered (X) by the sample.

of the incoming photons (excitation energy) from the energy of the emitted photons. The spectra are normalized to 300 mA of storage ring current and the number of counts is plotted versus the energy loss of the scattered photons. The counting time for each spectrum has been 30 min. Three principal types of photon-in–photon-out features can be distinguished in all spectra: The peaks of elastically scattered radiation, of inelastically scattered radiation, and of fluorescence radiation. The elastically scattered radiation appears at the energy of the exciting radiation, which corresponds to an

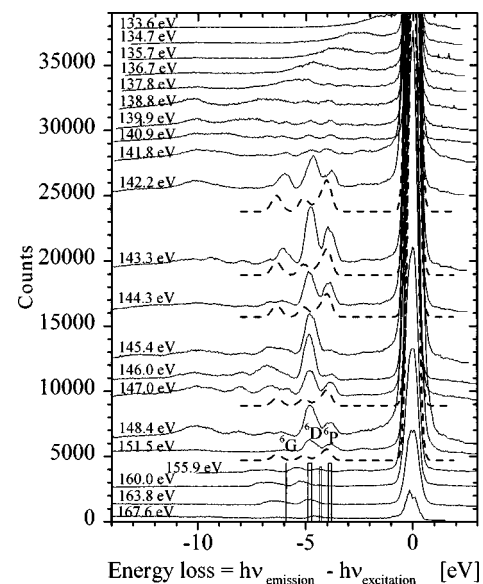


FIG. 2. Energy-loss spectra on $(\text{Y,Gd})_2\text{O}_3$ in the region through the $4d$ - $4f$ threshold. The excitation energy for the spectra is given above each spectrum. Calculated energetic positions for the terms that are assigned to the energy losses and represent excitations within the $4f$ shell ($4f^7$) are plotted as vertical bars.

energy loss of 0 eV (except for possible phonon losses of the order of a few meV). Due to the magnified scale, the elastic peaks are not fully displayed in Fig. 2. Therefore the maximum count rate in the elastic peak at each excitation energy is represented by an X in Fig. 1. The dotted curve in Fig. 1 is drawn through the experimental points to guide the eye. The energetic position of the main features is the same for the elastic scattering curve (dotted line) and the absorption curve (solid line). The $4d^9 4f^8 \rightarrow 4d^{10} 4f^7$ emission is maximal when the excitation energy is tuned to the 8P resonance in the absorption curve where the $4d$ hole is immediately refilled by the excited $4f$ electron as it scatters the incoming photon. The peak width for the elastic scattering curve is much smaller (3 eV) than the absorption curve (5.9 eV). The autoionization width found by Richter *et al.*⁴ is 5.2 eV. The different peak width is due to the different final states. The excited configuration ($4d^9 4f^8$) can decay via the main process, autoionization ($4d^9 4f^8 \rightarrow 4d^{10} 4f^6 + e^-$) that produces mostly $4f$ electrons,^{3,4} or via elastic scattering which leads to the final-state $3d^{10} 4f^7$. No core-valence transitions are involved.^{17,18}

Near threshold the decay of a core-hole state can be very different from the decay mechanisms at higher energies. Soft-x-ray emission and (radiationless) Auger-electron emission can appear as coherent one-step processes also known at the (resonance) Raman effect.⁵ The inelastic and elastic scattered intensity is described by the Kramers-Heisenberg (K-H) formula:¹⁹

$$I(E_{\text{in}}, E_{\text{out}}) \propto \sum_f \left| \sum_m \frac{\langle f | pA | m \rangle \langle m | pA | i \rangle}{E_m - E_i - h\nu_{\text{in}} - i\Gamma/2} \right|^2 \delta(E_f + h\nu_{\text{out}} - E_i - h\nu_{\text{in}}). \quad (1)$$

In this equation, pA is the dipole operator while $|i\rangle$ is the initial state of the system with energy E_i , $|m\rangle$ and E_m describe the intermediate state, $|f\rangle$ and E_f describe the final state, and Γ is the lifetime broadening in the intermediate state. The intermediate states correspond to $4d^9 4f^8$ 8D , 6D , and 8P resonance states and the energy loss can be assigned to the difference in energy between the initial and final state often designated as the ‘‘net transition.’’ At energies above threshold, the inelastic scattering evolves into fluorescence, and possible inelastic scattering produced by electron momentum scattering in the Brillouin zone, where soft-x-ray inelastic scattering has been used to elucidate band symmetries and probes specific regions of the Brillouin zone.^{6,20}

We have calculated the loss spectra from Eq. (1) using transition probabilities from the ground state to the intermediate states and back to the final metastable states obtained by Cowan’s method,²¹ summing incoherently over all the intermediate states of the $4d^9 4f^8$ configuration and using the same scaling for the Slater integrals as in Ref. 16.

An onset of three inelastic excitations at an excitation energy of about 139 eV is observed (Fig. 2). These features remain at a constant difference in energy relative to the elastic peak throughout the energy range of excitation. In Gd the $4f$ shell is half filled and the absence of valence band electrons in the vicinity of the Gd ion leads to a term scheme with only a few possible excitations. The next terms above the ground state ${}^8S_{7/2}$ belong to the sextet multiplet 6P_J ,

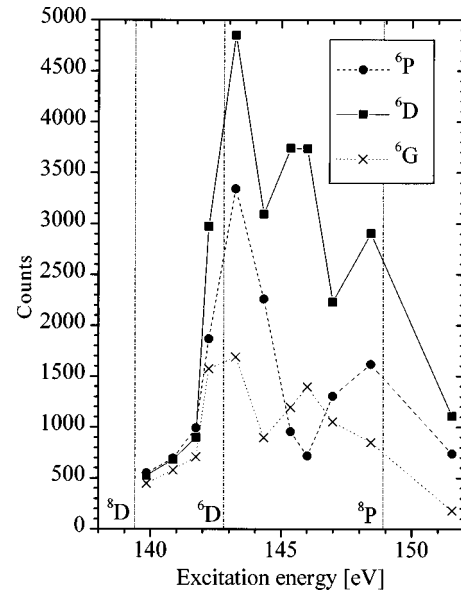


FIG. 3. Variation of the count rate in the inelastic scattering peaks with excitation energy. The curves represent the net transitions to the three final states 6P , 6D , and 6G . The vertical lines indicate the energetic position of the peaks in the absorption spectrum that correspond to the 8D , 6D , and 8P terms of the $4d^9 4f^8$ configuration.

6I_J , 6D_J , and 6G_J of the same electron configuration $4f^7$. The energetic positions of these states for $\text{Gd}^{3+}:\text{LaF}_3$ as calculated by Goodman and co-workers²² are plotted in Fig. 2. Optical and UV absorption spectroscopy data^{9–11} and calculations^{22,9,11} for Gd doped in various compounds show that the energetic differences in this term scheme for the different materials and their different crystal fields are smaller than 0.02 eV, which is small compared to our energy resolution (<0.4 eV). The width of the bars in Fig. 2 represents the energy range over which the various J levels extend for a given term. Reconfigurations within the $4f$ shell (‘‘ f - f transitions’’) by photon excitation are dipole forbidden due to the spin selection rule $\Delta S=0$ for L - S coupling. The inelastic scattering produces energy losses of less than 6 eV and is due to net transitions from the ${}^8S_{7/2}$ ground state (electron configuration $4d^{10} 4f^7$) to the sextet multiplets 6P_J , 6D_J , and 6G_J of the $4d^{10} 4f^7$ configuration. The transitions occur through the intermediate states 8D_J , 6D_J , and 8P_J ($4d^9 4f^8$) in the K-H cross section as shown in Eq. (1). Population of the 6I term of $4d^{10} 4f^7$ is not observed because of the large change in orbital momentum this transition would require. Different J levels of the final states are also not resolved. At excitation energies higher than the peak energy of the $4d$ - $4f$ excitation (149 eV), the inelastic processes become weaker (151.5 eV), shift in energy loss (above 155.9 eV), and finally disappear (167.6 eV). It is worth noticing that the partial cross sections for the three inelastic excitations behave differently. Only the strongest inelastic peak that comes from the excitation to the 6D state remains intense over an energy range of about 9 eV. At an excitation energy of about 156 eV the inelastic peaks become very weak and the magnitude of the energy loss changes.

While we observe intense elastic and elastic scattering as the photon energy is tuned to the $4d$ - $4f$ resonances

($4d^9 4f^8 \rightarrow 4d^{10} 4f^7$), we do not observe fluorescence at excitation energies above the $4d$ shell ionization threshold due to $4d^9 4f^7 \rightarrow 4d^{10} 4f^6$ transitions. This is expected because the partial cross section to produce a $4d$ hole is small⁴ and the $4d$ hole is filled by competing Auger processes with high probability. There is also no indication for a hole-induced shakedown process that has been observed by Okusawa *et al.*²³ in lanthanum. In this process, a band electron shakes down to the $4f$ level and is followed by $4d^9 4f^8 \rightarrow 4d^{10} 4f^7$ fluorescence emission. A weak fluorescence feature can be seen at an energy loss of 10 eV in the spectrum taken at 142.2 eV. With smaller excitation energy this peak shifts towards the elastic peak. We suggest that this weak fluorescence feature belongs to a charge-transfer state similar to that observed in La (Ref. 24) because Gd^{3+} does not offer transitions at this energy. We conclude that in the region of the giant resonance, autoionization and elastic scattering are the dominant interaction mechanisms. Inelastic scattering compared to elastic scattering is weaker by about one order of magnitude.

In Fig. 3 the count rate in each inelastic peak 6P , 6D , and 6G is plotted versus the excitation energy. We see that all the final states populated by Raman scattering are enhanced at the $4d^9 4f^8$ (6D) resonance. It is found that the inelastic scattering is maximal when the excitation energy is tuned to the intermediate state that is primarily of sextet symmetry. Thus many of the intermediate states which arise through intermediate rather than L - S coupling have a significant sextet rather than octet character. In this case the transition from

the intermediate state (6D) to the final states (6P , 6D , 6G) is dipole allowed.

To summarize, we have used high-resolution soft-x-ray emission spectroscopy with synchrotron radiation to study inner shell $4f$ excitations of Gd^{3+} in $(Y,Gd)_2O_3$. The soft x-ray emission spectra have been studied when exciting the $4d$ electrons selectively and strong inelastic features have been observed. According to our calculations, we interpret the energy losses as excitations within the $4f$ shell. The incident photons excite electrons from the ground state ${}^8S_{7/2}$ primarily to the intermediate state 6D_J and are inelastically scattered to the sextet final states $4d^{10} 4f^7$ (${}^8S_{7/2}$) $\rightarrow 4d^9 4f^8$ (6D_J) $\rightarrow 4d^{10} 4f^7$ (6P_J , 6D_J , 6G_J). The energy losses between 4 and 6 eV are due to net transitions from the octet ground state ${}^8S_{7/2}$ to the low-lying sextet terms of the $4f^7$ configuration 6P_J , 6D_J , and 6G_J . The relative cross sections of these ground-state-dipole-forbidden transitions have been obtained for the first time by the technique of soft x-ray scattering.

The authors would like to acknowledge helpful discussions with Dr. Eric Shirley. This work was supported by National Science Foundation Grant No. DMR-9017997, the Science Alliance Center for Excellence Grant from the University of Tennessee, and a DoE-EPSCor cluster research Grant No. DoE-LEQSF (1993-95)-03. The Advanced Light Source is supported by the office of Basic Energy Sciences, U.S. Department of Energy, under Contract No. DE-AC03-76SF00098.

- ¹T. M. Zimkina, A. S. Shulakov, A. P. Braiko, A. P. Stepanov, and V. A. Fomichev, *Sov. Phys. Solid State* **26**, 1201 (1984).
- ²T. M. Zimkina, A. S. Shulakova, V. A. Fomichev, A. P. Braiko, and A. P. Stepanov, in *International Conference on X-ray and Inner Shell Processes in Atoms, Molecules and Solids*, Conference Proceedings X84, edited by A. Meisel and J. Finster (Karl-Marx-Universitaet Leipzig, Leipzig, 1984).
- ³F. Gerken, J. Barth, and C. Kunz, *Phys. Rev. Lett.* **47**, 993 (1981); F. Gerken, Ph.D. thesis, HASYLAB/DESY, Hamburg, 1982.
- ⁴M. Richter, M. Meyer, M. Pähler, T. Prescher, E. v. Raven, B. Sonntag, and H.-E. Wetzel, *Phys. Rev. A* **40**, 7007 (1989).
- ⁵*Resonant Anomalous X-ray Scattering*, edited by G. Materlik, C. J. Sparks, and K. Fischer (Elsevier Science B.V., Amsterdam, 1994), and references therein.
- ⁶Y. Ma, *Phys. Rev. Lett.* **49**, 5799 (1994).
- ⁷S. M. Butorin, J.-H. Guo, M. Magnusson, P. Kuiper, and J. Nordgren, *Phys. Rev. B* **54**, 4405 (1996).
- ⁸J.-J. Gallet, J.-M. Mariot, C. F. Hague, F. Sirotti, M. Nakazawa, H. Ogasawara, and A. Kotani, *Phys. Rev. B* **54**, 14 238 (1996).
- ⁹R. L. Schwiesow and H. M. Crosswhite, *J. Opt. Soc. Am.* **59**, 592 (1969).
- ¹⁰R. L. Schwiesow and H. M. Crosswhite, *J. Opt. Soc. Am.* **59**, 602 (1969).
- ¹¹W. T. Carnall, P. R. Fields, and R. Sarup, *J. Chem. Phys.* **54**, 1476 (1971).
- ¹²R. E. La Villa, *Phys. Rev. A* **9**, 1801 (1974).
- ¹³J. J. Jia, T. A. Calcott, J. Yurkas, A. W. Ellis, F. J. Himpsel, M. G. Samant, G. Stöhr, D. L. Ederer, J. A. Carlisle, E. A. Hudson, L. J. Terminello, D. K. Shuh, and R. C. C. Perera, *Rev. Sci. Instrum.* **66**, 1394 (1995).
- ¹⁴A. Moewes, C. Kunz, and J. Voss, *Nucl. Instrum. Methods Phys. Res. A* **373**, 299 (1996).
- ¹⁵W. L. O'Brien, J. Jia, Q.-Y. Dong, T. A. Calcott, J.-E. Rubenson, D. L. Mueller, and D. L. Ederer, *Nucl. Instrum. Methods Phys. Res. B* **56/57**, 320 (1991).
- ¹⁶H. Ogasawara and A. Kotani, *J. Phys. Soc. Jpn.* **64**, 1394 (1995).
- ¹⁷J. A. Carlisle, E. L. Shirley, E. A. Hudson, L. J. Terminello, T. A. Calcott, J. J. Jia, D. L. Ederer, R. C. C. Perera, and F. J. Himpsel, *Phys. Rev. Lett.* **74**, 1234 (1995).
- ¹⁸Y. Ma, K. E. Miyano, P. L. Cowan, Y. Aglitzkiy, and B. A. Karlin, *Phys. Rev. Lett.* **74**, 478 (1995).
- ¹⁹See, e.g., J. J. Sakurai, *Advanced Quantum Mechanics* (Addison-Wesley, Reading, MA, 1967), Chap. 2; T. Aberg, *Phys. Scr.* **21**, 495 (1980); J. Tulkki and T. Aberg, *J. Phys. B* **15**, L435 (1982).
- ²⁰J. J. Jia, T. A. Calcott, E. L. Shirley, J. A. Carlisle, L. J. Terminello, A. Asfaw, D. L. Ederer, F. J. Himpsel, and R. C. C. Perera, *Phys. Rev. Lett.* **76**, 4054 (1996).
- ²¹R. D. Cowan, *The Theory of Atomic Structure and Spectra* (University of California Press, Berkeley, 1981).
- ²²W. T. Carnall, G. L. Goodman, K. Rajnak, and R. S. Rana, Argonne National Laboratory, Report No. ANL-88-8, 1988 (unpublished).
- ²³M. Okusawa, K. Ichikawa, O. Aita, and K. Tsutsumi, *Phys. Rev. B* **35**, 478 (1987).
- ²⁴D. R. Mueller, C. W. Clark, D. L. Ederer, J. J. Jia, W. L. O'Brien, Q. Y. Dong, and T. A. Calcott, *Phys. Rev. A* **52**, 4457 (1995).